

## Atomic-scale structural evolution of Ge(100) surfaces etched by H and D

Jun Young Lee,<sup>a)</sup> Soon Jung Jung, Jae Yeol Maeng, Young Eun Cho, and Sehun Kim

*Department of Chemistry and School of Molecular Science (BK21), Korea Advanced Institute of Science and Technology, Daejeon 305-701, South Korea*

Sam K. Jo

*Department of Chemistry, Kyung Won University, SungNam, KyungKi 461-701, South Korea*

(Received 18 February 2004; accepted 23 April 2004; published online 28 May 2004)

The atomic-scale structural evolution of Ge(100) surfaces etched by H(g) and D(g) at  $T_s=400$  K is studied using scanning tunneling microscopy (STM) and field emission-scanning electron microscopy (FE-SEM). The STM investigation reveals that etching of the Ge(100) by H(g) and D(g) proceeds initially via the production of single atom vacancies (SV), dimer vacancies (DV), and subsequently, line defects along the Ge dimer rows. It is also observed that D(g) etches the Ge(100) surface eight times faster than H(g) does. After extensive exposures of the surface to H(g), the FE-SEM images show square etch pits with V-groove shapes, indicating that H(g) etching of the Ge(100) surface proceeds anisotropically. © 2004 American Institute of Physics.

[DOI: 10.1063/1.1763635]

The interaction of hydrogen with semiconductor (100) surfaces has been of great technological interest in the field of semiconductor processing.<sup>1</sup> It is well known that etching of a Si(100) surface by atomic H(g) depends on the surface temperature  $T_s$ . Previous experiments have suggested that H etching of a Si(100) surface proceeds initially on the dihydride (1×1) surface:  $\text{H(g)} + \text{SiH}_2(\text{a}) \rightarrow \text{SiH}_3(\text{a})$ , followed by  $\text{H(g)} + \text{SiH}_3(\text{a}) \rightarrow \text{SiH}_4(\text{g})$ . H(g) breaks the Si–Si bonds of  $\text{SiH}_2(\text{a})$ , producing gas-phase  $\text{SiH}_4(\text{g})$  via successive H(g) additions.<sup>2</sup>

It has been generally believed, however, that atomic H(g) does not etch the surface of Ge(100), with even high H(g) exposures yielding only a stable monohydride (2×1) phase.<sup>3</sup> Recently, a scanning tunneling microscopy (STM) study has shown that this 2×1:H phase is largely maintained even after extensive H(g) exposure, due to the instability of the surface dihydride  $\text{GeH}_2(\text{a})$ .<sup>4</sup> To our knowledge, there have been no published reports to date on H etching of Ge(100) surfaces, though studies have been published for hydrogen etching on Ge/Si(100) surfaces.<sup>5</sup>

In this letter, we present an atomic-scale STM study of structural changes of Ge(100) surfaces etched by atomic H(g) and D(g) at  $T_s=400$  K. The variation of the surface morphology after extensive H(g) exposure was also investigated using field emission-scanning electron microscopy (FE-SEM). The etching rates of Ge(100) surfaces by H(g) and D(g) are compared.

The studies presented here were performed in an ultra-high vacuum chamber described in detail elsewhere.<sup>4</sup>

We note that hydrogen etching at  $T_s < 400$  K occurs randomly and forms large, irregular bright features ascribed to the etching intermediate,  $\text{GeH}_3(\text{a})$ ,<sup>4</sup> while for  $T_s > 400$  K the etching rate rapidly drops due to the difficulty of  $\text{GeH}_2(\text{a})$  formation.

Figure 1(a) shows the STM image of an initially etched

Ge(100)-2×1:D surface obtained after dosing 3000 L of  $\text{D}_2(\text{g})$ . Some bright ball-like features (<1%) are observed and distributed randomly over the surface. A prior study has indicated that these ball-like features are due to unpaired dangling bonds on dimers that are occupied by only a single D atom (D–Ge–Ge).<sup>4,6</sup> A significant number of such unpaired dangling bonds still persist even after prolonged D(g) exposure. A few atomic vacancies due to initial etching as well as antiphase boundaries are observed near local  $\text{GeD}_2(\text{a})$  rows. Figures 1(b)–1(d) show high resolution STM images of a single atom vacancy [SV, circle in Fig. 1(a)], single atom vacancy row [SVR, square in Fig. 1(a)], and dimer vacancy [DV, triangle in Fig. 1(a)] appearing after initial D etching. It is known that adjacent  $\text{GeH}_2(\text{a})$  species are precursors to breaking of the Ge–Ge bonds. The surface trihydride species,  $\text{GeH}_3(\text{a})$ , produced by H insertion into  $\text{GeH}_2(\text{a})$ , can be hydrogenated by H(g) and removed as  $\text{GeH}_4(\text{g})$ , as can shown by mass spectrometry.<sup>5</sup> Figure 1(e) shows a STM image of a Ge(100) surface exposed to  $7 \times 10^5$  L of  $\text{D}_2(\text{g})$ . In contrast to previous studies,<sup>3</sup> the STM image shows that significant etching by D(g) occurs on the Ge(100) surface. The STM images recorded with increasing D(g), and also of H(g), exposures reveal linear line defects formed along the Ge dimer rows. These STM results indicate that the  $\text{GeD}_2(\text{a})$  or  $\text{GeH}_2(\text{a})$  species on the Ge(100) surface are quite stable as etching precursors. However, even after extensive exposure of the Ge surface to D(g) or H(g), the large-scale 1×1 or 3×1 phases composed of  $\text{GeD}_2(\text{a})$  or  $\text{GeH}_2(\text{a})$  were not observed, unlike in the H/Si(100) case,<sup>2</sup> due to repulsion driven  $\text{H}_2(\text{g})$  or  $\text{D}_2(\text{g})$  desorption, as reported previously.<sup>4</sup>

Figure 1(f) shows the etching mechanism in which Ge dimers on a Ge(100) surface form  $\text{GeH}_2(\text{a})$  or  $\text{GeD}_2(\text{a})$  pairs and how these dihydride or dideuteride species desorb, generating SVs and subsequently DVs via successive H(g) or D(g) additions. However, recombinative  $\text{H}_2(\text{g})$  or  $\text{D}_2(\text{g})$  desorption, due to steric repulsion between the H or D atoms of two adjacent  $\text{GeH}_2(\text{a})$  or  $\text{GeD}_2(\text{a})$  species, may reduce the

<sup>a)</sup>Author to whom correspondence should be addressed; electronic mail: chemlee@kaist.ac.kr

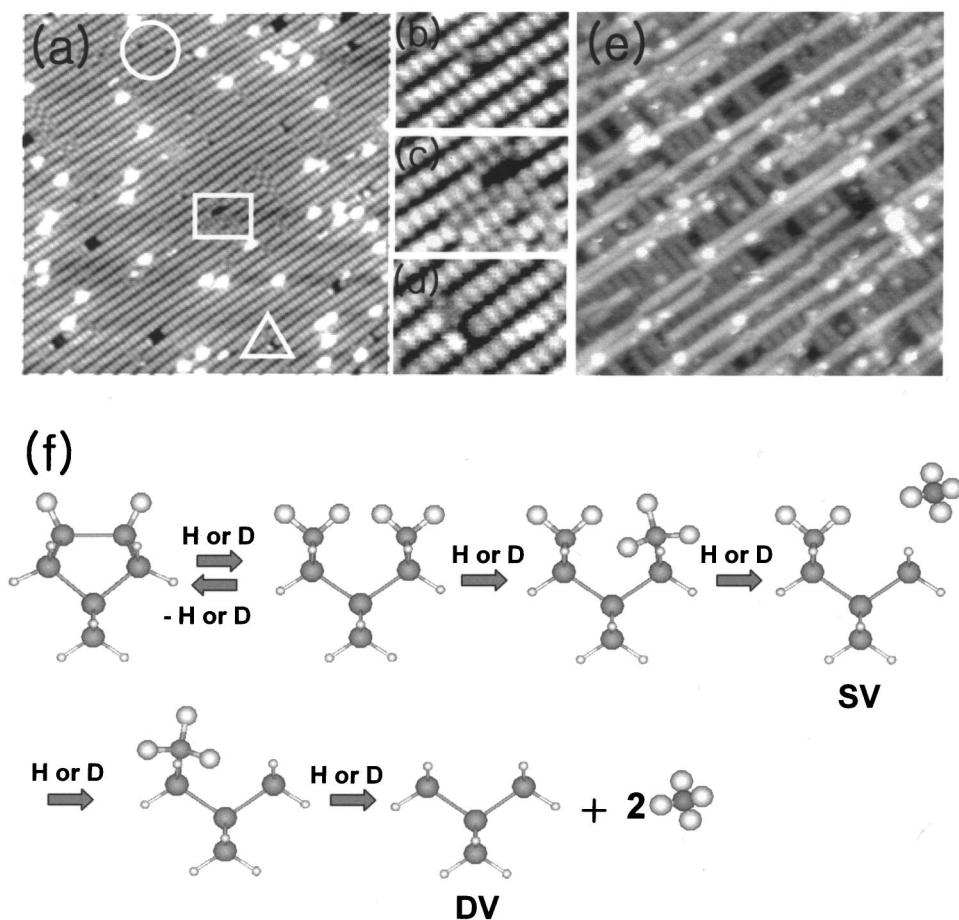


FIG. 1. Filled-state STM images ( $25 \times 25 \text{ nm}^2$ ) of a Ge(100) surface exposed with (a) 3000 L of  $\text{D}_2(\text{g})$  and (e)  $7 \times 10^5$  L of  $\text{D}_2(\text{g})$  at  $T_s = 400$  K. (b)–(d) show detailed STM images of a single atom vacancy (SV), single atom vacancy row (SVR), and dimer vacancy (DV), indicated by the circle, square, and triangle in (a). The etching mechanism is shown schematically in (f). The gray circles represent Ge atoms, and the white circles represent H or D atoms.

amount of  $\text{GeH}_2(\text{a})$  or  $\text{GeD}_2(\text{a})$  species on the surface by decomposition into  $\text{GeH}(\text{a})$  or  $\text{GeD}(\text{a})$  species. This indicates that the  $\text{GeH}_2(\text{a})$  or  $\text{GeD}_2(\text{a})$  species either quickly return to  $\text{GeH}(\text{a})$  or  $\text{GeD}(\text{a})$  by collision-induced  $\text{H}_2$  or  $\text{D}_2$  dissociation [ $2\text{GeH}_2(\text{a}) \rightarrow \text{H}-\text{Ge}-\text{Ge}-\text{H} + \text{H}_2(\text{g})$ ]<sup>4</sup> or etch the Ge surface by the adsorption of incoming  $\text{H}(\text{g})$  or  $\text{D}(\text{g})$  [ $\text{GeH}_2(\text{a}) + \text{H}(\text{g}) \rightarrow \text{GeH}_3(\text{a})$ , followed by  $\text{GeH}_3(\text{a}) + \text{H}(\text{g}) \rightarrow \text{GeH}_4(\text{g})$ ]. This DV then destabilizes adjacent dimers due to tensile stress. The incoming  $\text{H}(\text{g})$  or  $\text{D}(\text{g})$  attacks them and a pit grows as a string of DVs parallel to the dimer row by successive removal of neighboring dimers. In addition, regrowth features, expected by [ $\text{GeH}_3(\text{a}) \rightarrow \text{GeH}_2(\text{a}) + \text{H}(\text{a})$ ,  $\text{GeH}_2(\text{a}) \rightarrow \text{GeH}(\text{a}) + \text{H}(\text{a})$ ] at  $T_s = 400$  K, are also observed [the circle in Fig. 2(a)].<sup>7</sup>

Figures 2(a) and 2(b) show STM images of Ge(100) surfaces exposed to  $7 \times 10^5$  L of  $\text{H}_2(\text{g})$  and  $\text{D}_2(\text{g})$ , respectively. The areas of the etch pits produced by  $\text{H}(\text{g})$  and  $\text{D}(\text{g})$  etching occupy  $\sim 10\%$  and  $\sim 65\%$  of the whole surface area, respectively. The STM images in Figs. 2(a) and 2(b) reveal linear line defects formed along the Ge dimer rows. In these STM images, the etched surface area rapidly increases with increasing flux of  $\text{H}_2(\text{g})$  or  $\text{D}_2(\text{g})$ . Figure 2(c) shows the linear dependence of the etched monolayer (ML) of the Ge(100) surface on  $\text{H}_2(\text{g})$  and  $\text{D}_2(\text{g})$  exposure. The linear dependence is consistent with an etching reaction involving a direct attack of the Ge hydride or Ge deuteride species by  $\text{H}(\text{g})$  or  $\text{D}(\text{g})$  through the Eley–Rideal mechanism.<sup>5</sup> It can be seen

in Fig. 2(c) that the rate of etching of the Ge(100) surface by  $\text{D}(\text{g})$  is eight times faster than that by  $\text{H}(\text{g})$ , indicating that the formation of  $\text{GeH}_2(\text{a})$  as an etching precursor is more difficult than the formation of  $\text{GeD}_2(\text{a})$ . This is due to an isotope effect, as previously reported.<sup>8</sup> Specifically, the collision induced dissociation of  $\text{GeH}_2(\text{a})$  pairs occurs more easily than that of  $\text{GeD}_2(\text{a})$  due to the larger vibrational frequency of Ge–H compared with that of Ge–D.<sup>9</sup> Hence the efficiency of dry etching of a Ge(100) surface by  $\text{D}(\text{g})$  is greater than that by  $\text{H}(\text{g})$ .

We examined the surface morphology after extensive exposures of the Ge(100) surface to  $\text{H}(\text{g})$  using FE-SEM. Figure 3(a) shows a SEM image of a Ge(100) surface recorded after a  $\text{H}_2(\text{g})$  dosage of  $\sim 1 \times 10^6$  L at  $T_s = 400$  K. The SEM image reveals one of the square etch pits with a V-groove shape of size  $\sim 2 \times 2 \mu\text{m}^2$  found randomly distributed on the substrate. Rectangular etch pits are also observed. Similar etch pits are observed in wet and dry etching processes.<sup>10</sup> The shapes of the etch pits were expected to be limited by the planes with the lowest etching rate. It is known that (111) planes develop during anisotropic etching because of the lower etching rate of the (111) plane compared to other planes.<sup>10</sup>

Figure 3(b) shows a cross-sectional view of the etch pit with a V-groove shape seen in Fig. 3(a). The angle between the two faces of the etch pit is about  $55^\circ$  and the etch pit is bounded by a set of four (111) planes, as shown in the sche-

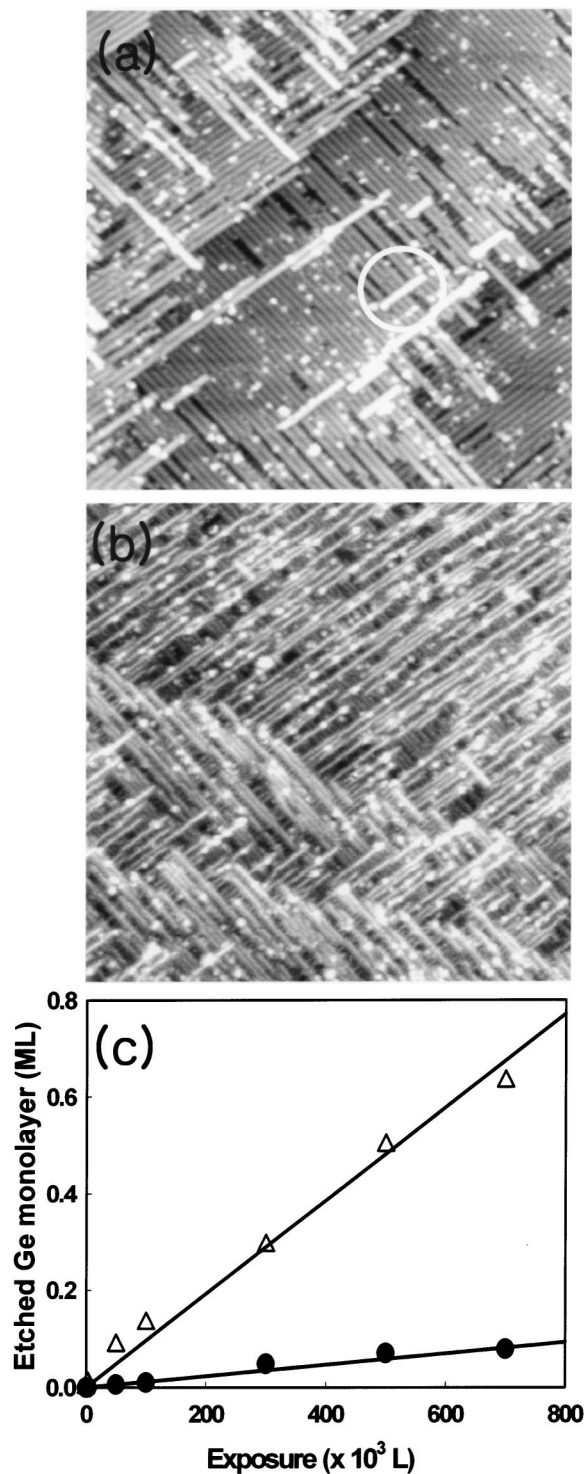


FIG. 2. Filled-state STM images ( $70 \times 70$  nm<sup>2</sup>) of Ge(100) surfaces exposed to (a)  $H_2(g)$  of  $7 \times 10^5$  L, and (b)  $D_2(g)$  of  $7 \times 10^5$  L at  $T_s = 400$  K. The circle in (a) shows a regrowth feature; (c) shows a plot of an etched Ge monolayer (ML) vs exposure (L) with  $H_2(g)$  and  $D_2(g)$ .

matic diagram of Fig. 3(c).<sup>11</sup> It is well established that the (111) face is generally the most stable because the Ge atoms on the (111) face are bonded to the surface by three Ge–Ge bonds. Insertion of a H atom into one of these bonds will greatly strain the remaining two bonds. However, on the (100) face, each Ge atom has two highly strained bonds to

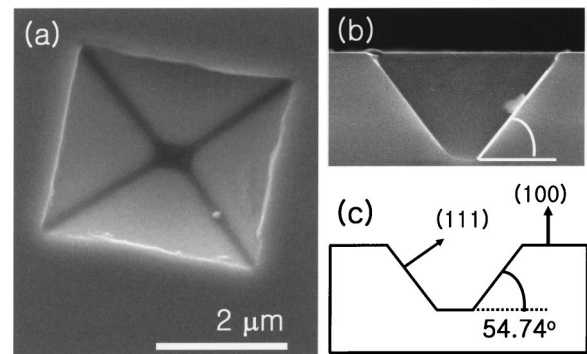


FIG. 3. FE-SEM images of (a) a typical etch pit of V-groove shape formed on a Ge(100) surface exposed to  $H_2(g)$  of  $\sim 1 \times 10^6$  L at  $T_s = 400$  K, (b) the cross sectional view of (a), and (c) a schematic diagram of (b) showing that the etch pits are bounded by a set of four (111) planes.

the surface. The repulsion resulting from the insertion of a H atom is relaxed by rotation about the remaining bond. The ability to stabilize such etch intermediates helps to promote the etching reaction on the Ge(100) surface. The results show that the H(g) etching of the Ge(100) surface is highly anisotropic, resulting in predominantly square etch pits with V-groove shapes.

In summary, the present STM studies show that etching of a Ge(100) surface by H(g) and D(g) at  $T_s = 400$  K proceeds initially by producing SVs and DVs. Etch pits of V-groove shape produced by anisotropic H(g) etching of the Ge(100) surface were observed. Compared to H(g), D(g) was found to etch the Ge(100) surface with greater etching efficiency.

This work was supported by grants from KOSEF through the Center for Nanotubes and Nanostructured Composites, the Brain Korea 21 Project, the Advanced Backbone IT Technology Development Project, and the National R&D Project for Nano Science and Technology.

<sup>1</sup>Hydrogen in Semiconductors: Bulk and Surface Properties, edited by M. Stutzmann and J. Chevallier (North-Holland, Amsterdam, 1991).

<sup>2</sup>J. Y. Maeng, S. Kim, S. Jo, W. P. Fitts, and J. M. White, Appl. Phys. Lett. **79**, 36 (2001); Y. Wei, L. Li, and I. S. T. Tsong, *ibid.* **66**, 1818 (1995); J. J. Boland, Phys. Rev. Lett. **65**, 3325 (1990).

<sup>3</sup>L. Surney and M. Tikhov, Surf. Sci. **138**, 40 (1984); Y. J. Chabal, *ibid.* **168**, 594 (1986).

<sup>4</sup>J. Y. Maeng, J. Y. Lee, Y. E. Cho, S. Kim, and S. Jo, Appl. Phys. Lett. **81**, 3555 (2002).

<sup>5</sup>S. I. Gheyas, T. Urisu, S. Hirano, H. Watanabe, S. Iwata, M. Aoyagi, M. Nishio, and H. Ogawa, Phys. Rev. B **58**, 9949 (1998); Y.-J. Zheng, P. F. Ma, and J. R. Engstrom, J. Appl. Phys. **90**, 3614 (2001).

<sup>6</sup>M. McEllistrem, M. Allgeier, and J. J. Boland, Science **279**, 545 (1998).

<sup>7</sup>Y. Wang, M. J. Bronikowski, and R. J. Hamers, Surf. Sci. **311**, 64 (1994); C. F. Herrmann and J. J. Boland, Phys. Rev. Lett. **87**, 115503 (2001).

<sup>8</sup>M. C. Hersam, N. P. Guisinger, J. Lee, K. Cheng, and J. W. Lyding, Appl. Phys. Lett. **80**, 201 (2002); J. Vac. Sci. Technol. B **14**, 707 (1996); S. Shimokawa, A. Namiki, M. N. Gammo, and T. Ando, J. Chem. Phys. **113**, 6916 (2000).

<sup>9</sup>P. Bratu, W. Brenig, A. Gross, M. Hartmann, U. Höfer, P. Kratzer, and R. Russ, Phys. Rev. B **54**, 5978 (1996); J. Y. Lee, J. Y. Maeng, A. Kim, Y. E. Cho, and S. Kim, J. Chem. Phys. **118**, 1929 (2003).

<sup>10</sup>I. Barycka and I. Zobel, Sens. Actuators, A **48**, 229 (1995); J. Am. Ceram. Soc. **77**, 2949 (1994).

<sup>11</sup>I. B. Kang, M. R. Haskard, and N. D. Samaan, Sens. Actuators, A **62**, 646 (1997).